

# Research on Automatic Liquid Level Measurement System for Nonferrous Metal Ingot Line

Fulai CAO<sup>a</sup>, Xiaomei YOU<sup>a,1</sup>, Long CUI<sup>b,c</sup> and Zhaoming LIU<sup>b,c</sup>

<sup>a</sup>*School of Mechanical Engineering, Shenyang LiGong University, Shenyang, Liaoning Province, 110159, P. R. China*

<sup>b</sup>*State Key Laboratory of Robotics, Shenyang Institute Of Automation, Shenyang, Liaoning Province, 110169, P. R. China*

<sup>c</sup>*Institutes for Robotics and Intelligent Manufacturing, Chinese Academy of Sciences, Shenyang 110169, China*

**Abstract.** Non-ferrous metals play an important role in the national economy, and more and more attention has been paid to their efficient large-scale production. However, the non-ferrous metal production plant environment is bad, the ingot line vibration is violent, the surface of the metal solution also has strong reflective, these adverse factors lead to the automatic detection of the level measurement process in the non-ferrous metal production is very difficult, have to retain a large number of manual links. In order to solve the above problems, an automatic measurement system of non-ferrous metal solution level based on structured light triangulation is established. The system adopts filtering algorithm based on statistics to suppress the adverse effect of ingot line vibration on measurement. At the same time, by increasing the Angle between the optical axis of the camera and the laser plane, the influence of the strong reflection of the solution surface on the measurement can be reduced. The relative error of the system can be controlled within 1.3%, which can meet the actual measurement demand in engineering.

**Keywords.** Laser triangulation, structured light, non-ferrous metal, strong reflective

## 1. Introduction

Nonferrous metals are important basic industrial raw materials. In recent years, with the increasing use of non-ferrous metal, its efficient mass production and preparation technology is more and more attention. However, at present, non-ferrous metal casting is still dominated by manual operation with a low degree of automation. The main bottleneck restricting its automatic production lies in the liquid level measurement in the casting process. Because of the violent vibration of the production line will cause the fluctuation of the liquid level of the metal solution and the strong reflective property of the metal solution, the traditional automatic measurement method can not be applied to the level measurement of the non-ferrous metal casting production. Due

---

<sup>1</sup> Xiaomei You, Corresponding author, School of Mechanical Engineering, Shenyang LiGong University, Shenyang, Liaoning Province, 110159, P. R. China; E-mail: prime\_queen@163.com

to the above actual working conditions, the current domestic level measurement method of nonferrous metal ingot line is very primitive, mainly using artificial eye observation and estimation. This method is poor precision, not only will lead to unstable product quality, but also damage workers' health, and even cause unnecessary material waste. Therefore, it is necessary to study a kind of automatic measurement system which can effectively deal with the fluctuation of liquid level and strong reflection of liquid level in the harsh working conditions of non-ferrous metal production.

At present, many methods of deep detection have been put forward in academia. Zhang Qihao, Wang Xiuyan, Kouskouridas et al used Harris-SIFT Angle point detection algorithm to extract feature information in the image obtained by monocular camera, and then obtained the actual depth of the object through convex hull calculation by comparing the feature information between image groups [1-2]. Wang Wei and Guo et al. used objects with motion parallax clue to measure depth, that is, feature extraction of images obtained by monocular camera, scale-invariant feature transformation algorithm, Graham scanning method to calculate the convex hull of matched feature points, and finally the depth was calculated by the straight line of the convex hull [3-5]. Xi Yunfei, Zhang Rugru, Wang Zaihuan et al., based on binocular vision, used the parallax of stereo image to calculate the target depth information in 3D modeling [6-8]. Song Lei et al. measured the target object from multiple perspectives in the binocular stereo measurement system, registered and joined the overlapping parts of the results of multiple measurements, and finally realized the three-dimensional measurement of the target object [9]. Canny algorithm [10] proposed by Canny edge extraction algorithm can be used to evenly extract the edge pixels of the target object in binocular stereo measurement as the points to be matched. Local traversal matching is used to match, and the image depth of the average matching point pair is used as the depth of the target object to complete 3d measurement. The illumination condition of the workshop of the non-ferrous metal ingot casting line is not ideal and the dust content in the air is high, so the method of direct measurement by monocular or multi-ocular camera cannot be adopted. In addition, the reflective property of the non-ferrous metal solution is strong, which is not conducive to the direct measurement by monocular or multi-ocular camera. The vibration of non-ferrous metal ingot production line during operation will make the metal liquid level fluctuate, so that the high precision depth sensor can not measure. On the other hand, the ambient temperature of the ingot production line is high, and the precision vision sensor cannot work in such harsh working conditions for a long time. Due to the practical disadvantages mentioned above, it is not suitable to use monocular or multi-ocular cameras directly and to use high-precision sensors to measure the metal liquid level.

In view of this, a non-contact measurement system is developed based on laser triangulation, which can meet the requirements of accuracy and adapt to working conditions. The system active laser projection was used to reduce the outside light and dust in the air to measure the impact of the reflective at the same time, according to the projection of the laser light to adjust the Angle of camera collection in measurement system to avoid the target surface reflective measurement error caused by the strong and the corresponding algorithm is designed to reduce the noise effects caused by solution of liquid surface ripples measurement problem. Due to the simple structure of the measuring system, the components of each part have good durability and heat resistance, and non-contact measurement, which can leave the liquid level for a long

distance, so the measuring system can keep the accuracy of the work in the high temperature near the ingot line for a long time.

## 2. Principle of Measurement

There are generally two methods of laser triangulation, namely, direct light source and oblique light source (figure 1 and figure 2).

This two ways to choose according to the reality of the actual needs, and installation conditions, due to the development of measurement system need to consider the amount of reflective laser in non-ferrous metal solution to adjust the camera Angle in the plane of the optical axis and light, in order to reduce the influence of solution of reflections on camera collection and convenience, to install the measurement system adopts direct type of figure 1.

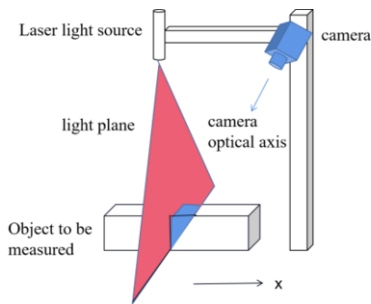


Figure 1. Direct shot.

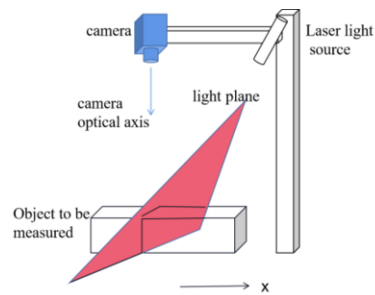


Figure 2. Oblique shot.

Four coordinate systems will be involved in the whole measurement system: world coordinate system, camera coordinate system, image coordinate system and pixel coordinate system.

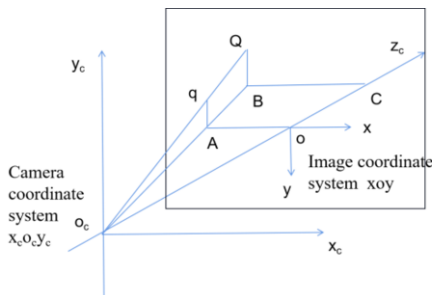


Figure 3. Conversion diagram from camera coordinate system to image coordinate system.

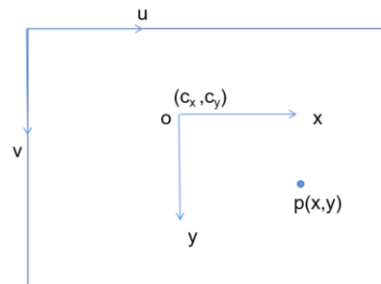


Figure 4. Image coordinate conversion pixel coordinate system.

The coordinates of point Q in figure 3 are  $(X, Y, Z)$ , which is located in the camera coordinate system. The coordinate system of point q is  $(x, y)$ , which is located in the

image coordinate system. Q is the two-dimensional projection of q on the image coordinate system, where focal length  $O_cO=f$ .

$$\begin{cases} \Delta CO_cQ \sim \Delta oO_cq \\ \Delta BO_cQ \sim \Delta AO_cq \end{cases} \tag{1}$$

According to Equation (1), it can be obtained:

$$\begin{cases} \frac{x}{f} = \frac{X}{Z} \\ \frac{y}{f} = \frac{Y}{Z} \end{cases} \Rightarrow \begin{cases} x = \frac{X}{Z}f \\ y = \frac{Y}{Z}f \end{cases} \tag{2}$$

According to Equation (2), it can be obtained:

$$\begin{bmatrix} x \\ y \\ 1 \end{bmatrix} = \begin{bmatrix} fx \\ fy \\ z \end{bmatrix} = \begin{bmatrix} f & & \\ & f & \\ & & 1 \end{bmatrix} \begin{bmatrix} 1 & & 0 \\ & 1 & 0 \\ & & 1 \end{bmatrix} \begin{bmatrix} X \\ Y \\ Z \\ 1 \end{bmatrix} \tag{3}$$

After obtaining the 2d coordinates of the target in the image coordinate system, it can be finally converted into the 2d coordinates in the pixel coordinate system, as shown in figure 4.

In figure 4, P (x,y) is a point in the image coordinate system (xoy), and its coordinate in the pixel coordinate system is (u,v).

$$\begin{cases} x = s_x(u - c_x) \\ y = s_y(v - c_y) \end{cases} \begin{cases} X = x \frac{Z}{f} \\ Y = y \frac{Z}{f} \end{cases} \tag{4}$$

Where,  $s_x$  and  $s_y$  are the proportional relations between the two corresponding coordinates of the same point in the image coordinate system and pixel coordinate system in the x direction and the y direction, respectively.  $c_x$  and  $c_y$  are the coordinates of the origin of the image coordinate system in the pixel coordinate system.

According to Equation (4), it can be obtained:

$$Z \begin{bmatrix} u \\ v \\ 1 \end{bmatrix} \Rightarrow \begin{bmatrix} f_x & & c_x \\ & f_y & c_y \\ & & 1 \end{bmatrix} \begin{bmatrix} R & T \\ O & 1 \end{bmatrix} \begin{bmatrix} X \\ Y \\ Z \\ 1 \end{bmatrix} \tag{5}$$

(Note:  $f_x$  and  $f_y$  are partial focal lengths on the X and Y axes respectively)

Finally, the 3d coordinates (X,Y,Z) of the actual point are obtained to the corresponding pixel coordinates (u,v), where:

$$\begin{bmatrix} f_x & c_x \\ & f_y & c_y \\ & & 1 \end{bmatrix} \quad (6)$$

Matrix (6) can be regarded as the internal parameter matrix of the camera, and (7) the R | T matrix can be seen as the camera external parameter matrix.

$$\begin{cases} f_x = \frac{f}{s_x} \\ f_y = \frac{f}{s_y} \end{cases} \begin{bmatrix} R & T \\ O & 1 \end{bmatrix} \quad (7)$$

In this paper, the direct measurement system shown in figure 1 will be used to build the measurement system. The industrial camera will collect the light projected onto the target surface and run the written algorithm to continuously calculate the actual coordinates of the target. Its principle is as follows:

$$\begin{cases} AX+BY+CZ+D=0 \\ X = s_x(u-c_x)\frac{Z}{f} \\ Y = s_y(v-c_y)\frac{Z}{f} \end{cases} \Rightarrow \begin{cases} Z = -\frac{Df}{As_x(u-c_x)+Bs_y(v-c_y)+Cf} \\ X = -\frac{Dx}{As_x(u-c_x)+Bs_y(v-c_y)+Cf} \\ Y = -\frac{Dy}{As_x(u-c_x)+Bs_y(v-c_y)+Cf} \end{cases} \quad (8)$$

Where  $AX+BY+CZ+D=0$  is the equation of the light plane generated by laser obtained by calibration before measurement, (u,v) is the coordinate of point P1 in the pixel coordinate system,  $(c_x,c_y)$  is the coordinate of the origin of the image coordinate system in the pixel coordinate system (generally, the length and width of the image are divided in half, namely  $(L/2,W/2)$ ), f is the focal length, Point (X,Y,Z) is the three-dimensional coordinate of space point P1 corresponding to pixel point P (u,v). Through the above method, we can get the actual three-dimensional coordinates of all points (P1, P2, P3.....Pn) on the line where the measured target intersects with the plane.

In order to make the measured target move uniformly in a straight line relative to the light plane, so that the light plane can completely sweep the measured object. When the light plane scans the measured target, we can get n intersecting lines of the surface of the measured target and the plane and the three-dimensional coordinates of all points on each intersecting line. All points on n intersecting lines can be combined to reconstruct the 3D model of the measured target surface and obtain the depth information of each point on the measured target surface.

When the three-dimensional coordinates of all points on the measured surface are obtained, the point cloud diagram of the measured target surface can be obtained. However, due to the liquid level ripples caused by the vibration of the ingot line, there will be some noisy point noise interference near the generated actual point cloud, affecting the final measurement result. In this paper, In this paper, the average value

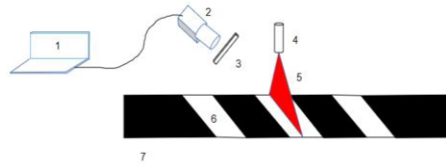
$d_{\text{mean}}$  of the sum of the distances from the 30 points of the Pni nearest neighbors of each point Pni in the measured target surface point set Q to Pni will be calculated, and the standard deviation  $\sigma$  within the range of the 30 nearest neighbor points of the calculated point Pni is as follows shown (n is the intersection line of the nth measured target surface and the light plane, i is the ith point on the intersection line).

$$\begin{cases} d_{\text{mean}} = (d_1 + d_2 + \dots + d_{30}) / 30 \\ \sigma = \frac{1}{n-1} \sqrt{\sum_1^n (d_i - d_{\text{mean}})^2} \end{cases} \quad (9)$$

### 3. Composition of the Liquid Level Measurement System

The measurement system built in this paper is mainly composed of 5 parts: a 3 million pixels industrial camera with a focal length of 6mm, a black electric conveyor belt with a length of 4.5m and a width of 400mm and a height of 75cm-100cm (simulating an ingot production line), a red laser light source, filter, computer.

The layout of the measurement system is shown in figure 5.



1-Computer; 2-Industrial camera; 3-Filter; 4-Laser light source; 5-Laser light plane; 6-Liquid metal; 7-Conveyor ingot production line.

Figure 5. Measurement System Structure Diagram.

### 4. Measurement Process

The abbreviated code process for this measurement experiment is as follows:

**Algorithm 1.** Non-ferrous metal solution level measurement  
 1: (CameraParams, CameraPose) ← CalibrateCamera;  
 2: (PoseL, PoseH) ← CalibraPose1;  
 3: (lightPlanePose) ← ComputeLightPose(PoseL, PoseH, CameraParams, ProfileL, ProfileH);  
 4: (PoseStart, PoseEnd) ← CalibraPose2;  
 5: (MovementPose) ← ComputeMovementPose(PoseStart, PoseEnd, PoseL);  
 6: (RoiRegion) ← GenerateRoi ;  
 7: (SheetOfLightMode) ← CreatSheetOfLightMode(RoiRegion, SetParams);  
 8: (SheetOfLightModeNew) ← SetSheetOfLightMode(Axis, Scale, CameraParams, PoseL, lightPlanePose, MovementPose);  
 9: Input(Profiles)  
 10: (SheetOfLightModeNew2) ← ComputeProfiles(Profiles);

```

11:  $Q=(p_1,p_2,p_3,\dots,p_n) \leftarrow \text{GetResult}(\text{SheetOfLightModeNew2});$ 
12:  $(d_{\text{mean}}, d_i) \leftarrow \text{ComputeDistance}(Q);$ 
13: if  $(d_i > d_{\text{mean}} + \sigma)$ 
14:    $Q' = (p'_1, p'_2, \dots, p'_n) \leftarrow \text{RemovePoint}(Q);$ 
15:  $H=(h_1, h_2, \dots, h_n) \leftarrow \text{GetHeight}(Q');$ 
16: Output= H

```

After the measurement system is built, before the formal measurement, 20 calibration images need to be used to calibrate the industrial camera to obtain the camera's internal parameters and initial camera external parameters, such as Algorithm 1; An image of the calibration board at different heights (at the low point and the high point) in the same light plane and the contours of the two light strips on the calibration board at the corresponding heights. According to the two calibration images and the contours of the light strips, an algorithm is used to fit the position of the light plane. In Algorithm 4-5, according to the frame rate of the industrial camera to calculate the displacement of the same position on the conveyor belt moving at a constant speed when the camera continuously collects 100 pictures, and collect the data at the starting position and the ending position respectively. To calibrate the image, by calibrating the starting position and ending pose of the object to be measured, the initial motion pose and motion end pose are obtained, and then the motion initial pose and motion end pose are converted into affine matrices relative to the camera coordinate system respectively. after the camera pose is also converted into the affine matrix of the camera relative to the world, according to the above three matrices, the affine matrix of the start position and the end position relative to the world can be obtained respectively, using these two matrices can be obtained The actual pose of the starting point position and the key position relative to the world, and then the difference between the two poses relative to the world coordinate system and divided by (100-1), and finally the pose of the movement direction is obtained.

Algorithm 6 is based on The range of measurement determines the ROI area of interest; next, a measurement model framework is created, and the previously determined ROI area, the camera's inner blend, the fitted light plane pose, the pose of the motion direction, and the camera's external parameters (here Use the pose at the low point) and the set threshold for extracting rays, set it to the model, and then scan the surface of the measured target with the input light plane to obtain the intersecting ray profile, then you can calculate the relative point of the measured target surface (point set Q) relative to The three-dimensional coordinates at the low point, as in Algorithm 7-12; in calculating the distances ( $d_1, d_2, \dots, d_{30}$ ) of each point in the point set Q to the 30 points in the nearby neighborhood ( $d_1, d_2, \dots, d_{30}$ ), and solve their average Value  $d_{\text{mean}}$ , calculate the standard deviation of the point p and the 30 points in the field. If the distance between the point in the neighborhood and the point p is greater than  $d_{\text{mean}} + \sigma$ , remove the point, and traverse the point set Q according to this method. For each point, the interference points in the point set can be removed to obtain the point set Q', which can improve the accuracy of anti-interference, such as algorithm 13-14; finally, the Z coordinate of each point in the point set Q' can be extracted, which is the measured target Height information H of each point on the surface, as in Algorithm 15-16. Afterwards, the height information can be sent to the robotic arm through PLC as required.

## 5. Experimental Results and Analysis

The measurement system in this paper simulates the measurement of the non-ferrous metal solution (silver zinc metal solution) at different angles between the optical axis of the camera and the laser plane, and uses the algorithm to filter the noise. The results are as follows.

Figure 6 shows the non-ferrous metal solution ingot production line in the actual production workshop. Due to the reasons described in the text, the actual ingot production line does not have automatic measuring equipment, and mainly relies on manual observation. Figure 7 is a simulated reconstituted zinc metal level in an ingot tank with an actual level of 10.0 cm.



**Figure 6.** Zinc in grooves on an actual production line.

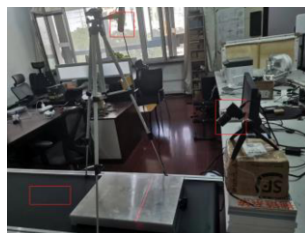


**Figure 7.** Simulation experiment platform.

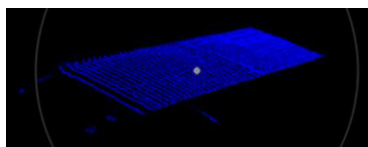


**Figure 8.** Reconstructed point map with unfiltered noise.

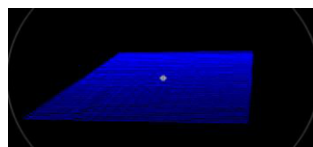


**Figure 9.** Reconstructed dot plot of filtered vibration noise.

It can be seen from figure 8 and figure 9 that under the working conditions of the production line vibration, the use of the measurement system and filtering algorithm in this paper can effectively eliminate the interference points caused by vibration, so that the measurement system proposed in this paper has a better effect on the vibration of the environment. Resistance (for the filtering algorithm principle of the measurement system, see the measurement principle section in the text).

**Table 1.** Statistical table of liquid level measurement results.

The Angle between the laser plane and the camera axis /deg	Height mean /cm	Standard deviation /cm	Relative error
25	10.76	0.423	7.6%
35	10.54	0.374	5.4%
45	9.83	0.303	1.7%
55	10.13	0.122	1.3%
60	/	/	error

When the light emitted by the laser irradiates the surface of the object to be measured as shown in figure 10, the amount of light reflected from the surface of the object to be measured will gradually decrease with the increase of the angle deviated from the laser. Therefore, in order to reduce the influence of the strong reflectivity of the non-ferrous metal solution on the measurement system, the influence of the test on the final measurement accuracy is changed by changing the angle between the light plane emitted by the laser and the optical axis of the camera in the measurement system. The results are shown in table 1. The larger the angle between the light plane emitted by the laser and the optical axis of the camera, the smaller the error of the measurement system and the higher the accuracy. It will not be possible to collect the complete light strip profile, and eventually the 3D point map of the surface to be measured cannot be reconstructed. Therefore, considering the angle between the two, 55 degrees is the best, which can reduce the reflectivity of the surface of the measured object. Excessive intensity causes the reflected light to be too large to adversely affect the measuring system.

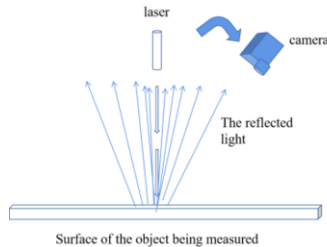


**Figure 10.** The surface light reflection diagram of the measured object.

## 6. Conclusion

It is aimed at the situation that the actual working conditions in the domestic non-ferrous metal production workshop are harsh, the production line is prone to vibration, and the measured target has a strong reflective non-ferrous metal solution. In this paper, a measurement system that is simple to install and debug, adapts to harsh working conditions, and can still maintain a certain precision under the interference of the strong reflectivity of non-ferrous metal solutions and the vibration of the ingot line is developed. It can be seen from the above experimental results that the filtering algorithm designed by the system has a good effect of removing noise caused by vibration; when the measured target is a highly reflective non-ferrous metal solution, by increasing the angle between the optical axis of the camera and the laser plane can effectively reduce the interference of the strong reflectivity of the non-ferrous metal solution. The comparison between the measurement system and the experiment shows that the best effect is when the angle between the optical axis of the camera and the laser plane reaches 55 degrees, and the relative error can be controlled within 1.3%. Therefore, the measurement system developed in this paper can lay a foundation for the engineering practice application in the non-ferrous metal ingot industry, and improve the measurement accuracy and reliability of the non-ferrous metal ingot line.

## Acknowledgement

This project was supported by National Key R&D Program of China (No. 2018YFB1309001). The authors gratefully acknowledge the support of National Natural Science Foundation of China (No. 92067205).

## References

- [1] Zhang QC, Qiao ZW. Absolute depth measurement of objects based on monocular vision. *Electronic Measurement Technology*. 2020; 43(20):74-78.
- [2] Wang XY, Cheng TT. Research on target recognition of industrial robot based on monocular vision. *Machinery Design & Manufacture*. 2011; (4):155-157.
- [3] Wang WW, Liang FM, Wang LL. Monocular depth measurement using motion cues. *Journal of Image and Graphics*. 2020; (3):468-475.
- [4] Guo R, Shen X, Kang H. Image segmentation algorithm based on partial differential equation. *Journal of Intelligent and Fuzzy Systems*. 2020; 38(2):1-7.
- [5] Tsai YM, Chang YL, Chen LG. Block-based Vanishing Line and Vanishing Point Detection for 3D Scene Reconstruction. *Proceeding of International Symposium on Intelligent Signal Processing & Communications*. IEEE, 2013.
- [6] Xi YF, Wu S, Xu J. IC board depth measurement based on binocular stereo vision. *Manufacturing Automation*. 2020; (5):129-132.
- [7] Zhang RR, Ge GY, Sheng Z, etc. Measuring dimension of parts of binocular vision based on halcon. *Computer Measurement & Control*. 2018; (1):59-63.
- [8] Wang ZH, Qu SR. Create a projected view of an object using binocular depth sounding. *Machinery Design & Manufacture*. 2005; (10):158-159.
- [9] Song L. Research on multi-view depth map registration method in binocular stereo measurement system. Nanjing University of Aeronautics and Astronautics, China. 2010.
- [10] Canny J. A computational approach to edge detection. *IEEE Transactions on Pattern Analysis and Machine Intelligence*. 1986; PAMI-8(6):679-698.